Local structure of $(Ge_4Si_4)_5$ monolayer strained-layer superlattice probed by fluorescence x-ray absorption fine structure

Shiqiang Wei,[1,*] Hiroyuki Oyanagi,[1] K. Sakamoto,[1] Y. Takeda,[2] and T. P. Pearsall[3]

[1]*Electrotechnical Laboratory, 1-1-4 Umezono, Tsukuba, Ibaraki 305-8568, Japan*

[2]*Department of Materials Science and Engineering, Nagoya University, Nagoya 464-01, Japan*

[3]*LERF, CORNING, S4, 7-bis Avenue de Valvins, 77210 Avon, France*

(Received 1 September 1999; revised manuscript received 28 February 2000)

Local structure of $(Ge_4Si_4)_5$ monolayer strained-layer superlattice (MSLS) on Si(001) has been studied by grazing-incidence fluorescence x-ray absorption fine structure. The observed Ge-Ge and Ge-Si bond lengths, $R_{Ge\text{-}Ge}$ (2.42 Å) and $R_{Ge\text{-}Si}$ (2.38 Å), indicate that the mismatch strain in $(Ge_4Si_4)_5$ MSLS is accommodated by both bond compression and bond bending in the (Ge_4) layer. The result rules out a possible model structure featuring fully relaxed $R_{Ge\text{-}Ge}$ leading to the direct $\Delta_v - \Delta(X_{cl})$ transition as an origin of 0.75-eV optical transition. The determined Si/Ge coordination numbers for $(Ge_4Si_4)_5$ MSLS ($N_{Si}:N_{Ge}=2.2:1.8$) deviate from that of an ideal interface model ($N_{Si}:N_{Ge}=1:3$), which indicates a substantial interface mixing. A simple mechanism of intermixing via site exchange and surface segregation is proposed.

I. INTRODUCTION

Artificially ordered GeSi superlattices possessing electrical and optical properties have opened a doorway to band-structure engineering through heterostructures formed by the strained-layer coherent epitaxy of Si and Ge.[1,2] The $(Ge_4Si_4)_5$ monolayer strained-layer superlattice (MSLS) grown on Si(001) substrate, has shown strong optical transitions (0.75, 1.25, 2.31 eV) unique to the superlattice period, which are found neither in constituent crystals nor in the $Ge_{0.5}Si_{0.5}$ alloy.[3] In order to understand the nature of GeSi MSLS quantum wells expected to have significant modifications in the optical and electrical properties, a number of studies on the electronic properties, growth, structure, and stability of the strained GeSi MSLS and Ge_xSi_{1-x} alloys have been performed.[4–16]

In the early stage,[3,4,7] optical transitions have been studied for Ge_nSi_n ($n=1,6$) MSLS and Ge_xSi_{1-x} alloys with electroreflectance spectroscopy. The results demonstrated that both Ge_1Si_1 and Ge_6Si_6 prepared on Si(001) substrates show the electroreflectance spectra similar to random $Ge_{0.5}Si_{0.5}$ alloy, whereas those for Ge_2Si_2 and Ge_4Si_4 show significant difference from that of $Ge_{0.5}Si_{0.5}$ alloy. In particular, for $(Ge_4Si_4)_5$/Si(001), new optical transitions have been resolved at energies that cannot be explained by a simple combination of those for crystalline Ge or Si. People and Jackson have pointed out that the lowest-lying states in the conduction band are derived from the (100) valleys of Si.[17] This picture has been supported by the band calculations based on ideal superlattice model.[10,18,19] However, the magnitude of the calculated matrix elements for the new transitions are several orders lower than what is observed in the experiment. On the other hand, the band calculations that take account of the deviations from an ideal superlattice result in optical transition matrix elements that are in better agreement with experimental results.[9,20]

Quantitative calculations of optical transition require direct information on structural parameters for GeSi MSLS,

not only in crystallographic (average) but also local structural viewpoints. However, the local structures around Ge and Si atoms have not been measured for $(Ge_4Si_4)_5$ MSLS. This is partly due to the fact that the MSLS prepared on thick substrates is impossible to be studied by a conventional transmission experiment, although x-ray absorption fine structure (XAFS) is an ideal technique for a local structure study. More recently, the surface sensitivity of XAFS experiments has been significantly improved by a grazing-incidence fluorescence excitation and a high-efficiency x-ray detector. In fact, submonolayer sensitivity has been achieved.[21,22] Using this technique, we have studied the local structure of epitaxial Ge overlayers on well-oriented Si(001), $[Ge_n/Si(001), \ n<7]$,[11,23] and $[Si/Ge_n/Si(001), \ n<12]$.[24]

In this paper, we report the local structure around Ge atoms in $(Ge_4Si_4)_5$/Si(001) MSLS using grazing-incidence fluorescence XAFS. The results are discussed in relation to the strain accommodation and relaxation in the Ge layers which have been a subject of numerous studies of GeSi alloys.[12–15,25–30] Our results on MSLS show that the Ge layers are tetragonally deformed and the lattice matching is mostly achieved by bond bending (75%) with a minor contribution of bond compression (25%). The bond length values are essentially similar to those in strained Ge_xSi_{1-x} thin films with an average composition of $x\sim0.5$ but slightly more compressed (0.6%), indicating a highly compressed state of the (Ge_4) layer. This provides important information on a possible nature of optical transition, in particular, a fully relaxed Ge layer model proposed by Wong *et al.*[9] Furthermore, the coordination geometry around Ge atoms indicates an appreciable amount of interface mixing. A simple model is proposed to take into account both overlayer-substrate site-exchange (during the growth of Ge layer on Si layer) and surface segregation (during the growth of Si layer on Ge layer).

II. EXPERIMENT

$(Ge_4Si_4)_5$ MSLS was prepared on Si(001) substrate in an ultrahigh vacuum (UHV) molecular-beam epitaxy (MBE)

growth chamber with a base pressure of 2×10^{-11} Torr. The detail of MSLS sample preparation is reported elsewhere.[31] The substrate was cleaned by the Shiraki method prior to the deposition. A 1000-Å-thick buffer layer was deposited at a substrate temperature of 600–700 °C. The Ge-Si multilayers were grown at 480–530 °C. The 140 Å-thick Si cap layer was grown to protect MSLS for XAFS experiments from oxidation while the samples for electroreflectance[31] were covered by 1000-Å-thick Si cap layer. The structure of the GeSi MSLS was analyzed *in situ* by reflection high-energy electron diffraction. $Ge_x Si_{1-x}$ alloy thin films were prepared on Si(001) by MBE in another growth chamber. After removing protective oxide layers from the Si(001) substrate by heating at 800 °C, Si buffer layer was grown at 500 °C.[32] The growth of GeSi layers was performed at 400 °C. A typical growth rate was 0.3 and 0.1 Å/sec for Si and Ge deposition, respectively. The film thickness of $Ge_{0.05}Si_{0.95}$ and $Ge_{0.5}Si_{0.5}$ alloys was 1000–2000 Å.

The grazing-incidence fluorescence yield spectra were recorded for $(Ge_4Si_4)_5$ MSLS and $Ge_x Si_{1-x}$ alloys on Si(001), while transmission spectra were taken for crystalline c-Ge. All measurements were performed at the BL-13B at the Photon Factory, National Laboratory for High Energy Physics (PF, KEK). The incidence angle for fluorescence-detected XAFS measurements was chosen so that the contribution of substrate Si is minimized, i.e., the strong diffraction does not affect the linearity of an x-ray detector. The electron beam energy was 2.5 GeV and the maximum stored current was 400 mA. A 27-pole wiggler with the maximum magnetic field B_0 of 1.5 T inserted in the straight section of the storage ring was used. The calculated total power of the wiggler was 5.44 kW at $B_0 = 1.5$ T, with which the brilliance greater than that of a bending magnet by an order of magnitude can be obtained over a wide energy range (4–30 keV). XAFS data were collected using a fixed-exit double-crystal Si(111) monochromator. The first crystal is a water-cooled flat Si(111) crystal[33] while the second crystal is sagittally bent to focus the horizontal beam over ~2 mrad. A seven-element Si(Li) solid-state detector array was used to collect the fluorescence signal. The average energy resolution of each Si(Li) element with an active area of 200 mm^2 was 240 eV at 5.9 keV, using a shaping time of 6 μsec. The detector output was linear below 2.5×10^4 cps after a simple correction of dead time. For each data point, the signal was integrated for 10 sec and ten scans were averaged.

In a grazing-incidence geometry, the background caused by elastic scattering is significantly suppressed and further rejection was done by a combination of an x-ray filter (Ga oxide) and an energy analysis so that a fluorescence yield can be obtained with a high signal-to-background ratio (~10^2) for 1 ML Ge.[11] The energy window of the detector electronics for each channel was chosen to record only the Ge $K\alpha$ peak. In this experiment, the incidence angle was chosen so that the diffractions from substrate do not affect the detector linearlity above the critical angle (3.5 mrad).

III. RESULTS

The Ge K-edge x-ray absorption near-edge structure (XANES) are plotted in Fig. 1 for $(Ge_4Si_4)_5$ MSLS (top column), $Ge_{0.5}Si_{0.5}$Si(001) (middle), and $Ge_{0.05}Si_{0.95}$/
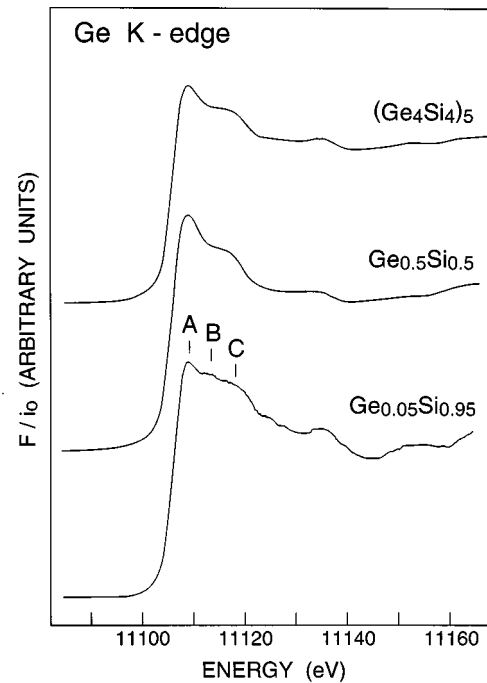

FIG. 1. X-ray absorption near-edge structure (XANES) for $(Ge_4Si_4)_5$ MSLS (top), $Ge_{0.50}Si_{0.50}$ (middle), and $Ge_{0.05}Si_{0.95}$ (bottom) alloys, *A, B,* and *C* indicate the characteristic features.

Si(001) (bottom). The sharp ''white line'' peak shows fine features *A, B,* and *C* for Si-rich GeSi alloy $(Ge_{0.05}Si_{0.95})$. Feature *A* is enhanced while the peak is narrowed in width making it difficult to resolve *B* and *C* on going to higher Ge concentration. The low-k extended x-ray absorption fine structure EXAFS region (11140–11160 eV) reflects the profile of back scattering amplitude of coordinated atom. The white line peak profile and the low-k EXAFS region for $(Ge_4Si_4)_5$ MSLS are similar to that of $Ge_{0.5}Si_{0.5}$, indicating that the average Ge composition of MSLS is close to that of $Ge_{0.5}Si_{0.5}$ although the intensity of feature *A* is suppressed.

Figure 2 illustrates the normalized Ge K-edge EXAFS oscillations $k\chi(k)$ as a function of photoelectron wave number k, in the k range of 2–18 Å^{-1} for c-Ge (powder crystal), $Ge_x Si_{1-x}$ alloys, and $(Ge_4Si_4)_5$ MSLS. It can be clearly seen that $k\chi(k)$ of c-Ge has a maximum in the region of $k = 6$ Å^{-1} showing a gradual decrease in magnitude, which is
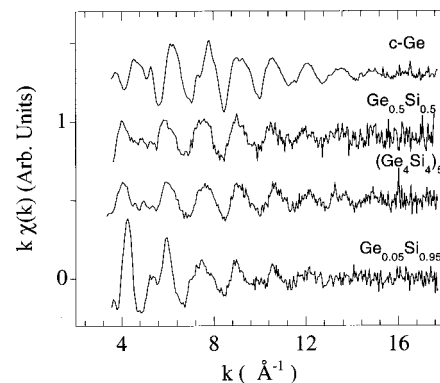

FIG. 2. Normalized EXAFS oscillations $k\chi(k)$ for crystalline Ge, $Ge_{0.50}Si_{0.50}$ alloy, $(Ge_4Si_4)_5$ MSLS, and $Ge_{0.05}Si_{0.95}$ alloy prepared on Si(001) as a function of photoelectron wave number Å^{-1}.
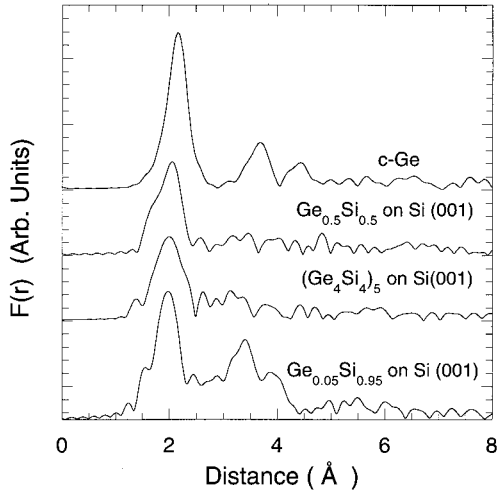
FIG. 3. Fourier transform of EXAFS oscillations $k\chi(k)$, $|F(R)|$, for $(Ge_4Si_4)_5$ MSLS, crystalline Ge, $Ge_{0.50}Si_{0.50}$, and $Ge_{0.05}Si_{0.95}$ alloys.
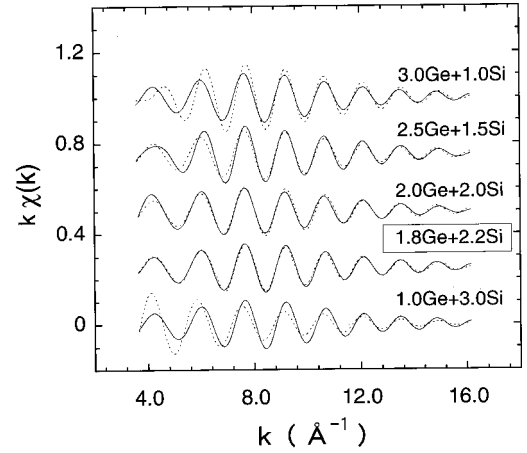

FIG. 4. Experimental first-shell EXAFS oscillations $k\chi(k)$ for $(Ge_4Si_4)_5$ MSLS (solid line) and simulated curves for model structures with various for N_{Ge}/N_{Si} ratio based on a tetrahedral geometry (dashed line). Results with $N_{Ge} = 1.8$, $N_{Si} = 2.2$ indicate the best-fit data allowing all structure parameters for the two shells (Ge-Ge and Ge-Si) to vary while other data are calculated for intentionally modified N_{Ge}/N_{Si} ratio using the same bond length and MSRD values.

a common feature of Ge scatterer. In contrast, in Si-rich alloy, i.e., $Ge_{0.05}Si_{0.95}$/Si(001), the low k-region around $k = 4$ Å^{-1} has a large magnitude that sharply decreases on going to a high-k region. EXAFS spectra for both $(Ge_4Si_4)_5$ MSLS and $Ge_{0.5}Si_{0.5}$/Si(001) have an intermediate profile suggesting that these two samples are characterized by an almost equal amount of Ge and Si scatterers, in agreement with XANES observations.

The results of Fourier transform (FT) of EXAFS oscillations $\chi(k)$ multiplied by k, representing the radial distribution function (RDF), are shown in Fig. 3. We note that the peak positions in the FT results are shifted to a smaller R because of a phase-shift effect. The FT magnitude for c-Ge shows a characteristic feature of a diamond-type tetrahedral structure T_d up to the third-nearest neighbor. These features are essentially the same as those for $Ge_{0.05}Si_{0.95}$/Si(001) with a shorter interatomic distance. Compared with the results for c-Ge, the magnitude of the prominent peak for $(Ge_4Si_4)_5$ MSLS decreased by about 50% shifting toward a smaller distance direction by 0.16 Å. The second- and third-nearest-neighbor peaks in the RDF for $(Ge_4Si_4)_5$ MSLS are not well resolved. Upon comparing the RDF's for $(Ge_4Si_4)_5$ MSLS and $Ge_{0.5}Si_{0.5}$/Si(001) as shown in Fig. 3, one can notice that smearing is due to the interference between Ge-Ge and Ge-Si pairs. In fact, Kajiyama et al.[28] and Aldrich, Nemanich, and Sayers[12] reported that no evident second- and third-nearest-neighbor peaks appear for the re-

laxed crystalline $Ge_{0.61}Si_{0.39}$ and $Ge_{0.59}Si_{0.61}$ alloys.

In order to obtain the structural parameters for the nearest neighbor of Ge atoms, the RDF's for all samples were inversely transformed into a k space to isolate the first shell contribution. The least squares curve fitting based on Marquardt's scheme for iterative estimation of nonlinear least-squares parameters via a compromise combination of gradient and Taylor series method[34] was used to fit the filtered EXAFS oscillations in a k space. The contribution of the Ge-Ge and Ge-Si pairs can be separated in a k space because the k dependencies of the total phase-shift and backscattering amplitude functions for Ge and Si are quite different: $|f_{Si}(k,\pi)|$ peak is located at low k and falls off sharply with the increase of k while $|f_{Ge}(k,\pi)|$ has a maximum at $k = 6-8$ Å^{-1} and extends to a region with $k > 15$ Å^{-1}. The theoretical amplitude function $|f_j(k,\pi)|$ and phase-shift function $\Phi_{ij}(k)$ were obtained by FEFF7.[35,36] The fitting results are summarized in Table I. The first-shell EXAFS oscillations were calculated for several model structures for $(Ge_4Si_4)_5$ MSLS with various N_{Ge}/N_{Si} ratio and compared with the experimental curve in Fig. 4. In this simulation, the Ge-Ge and Ge-Si distances separately determined by a least-squares fit were used and only the ratio of GeSi coordination number is varied keeping the total coordination number (4).

TABLE I. Structural parameters of Ge/Si samples obtained from XAFS data.

Sample	Bond pair	R (Å)	N	σ (Å)	ΔE_0 (eV)
$(Ge_4Si_4)_5$Si(001)	Ge-Ge	2.42±0.01	1.8±0.2	0.062±0.005	6.5±1.0
	Ge-Si	2.38±0.01	2.2±0.2	0.068±0.005	4.5±1.0
$Ge_{0.5}Si_{0.5}$ alloy	Ge-Ge	2.43±0.01	2.0±0.2	0.058±0.005	7.0±1.0
	Ge-Si	2.38±0.01	2.0±0.2	0.050±0.005	3.8±1.0
$Ge_{0.05}Si_{0.95}$ alloy	Ge-Si	2.35±0.01	4.0±0.2	0.045±0.005	4.5±10
	Ge-Ge		~0		
c-Ge	Ge-Ge	2.45±0.01	4.0±0.2	0.054±0.005	8.0±1.0

$(Ge_4Si_4)_5$

a　　　　　SIDE VIEW

Si

Ge

Surface segregation (1 ML)

Site-exchange (0.5 ML)

Ideal interface　　　　Model interface

b　　　　TOP VIEW

(a)

N~3.0Ge+1.0Si

(b)

N~1.5Ge+2.5Si

(c)

N~1.75Ge+2.25Si

(d)

N~1.75Ge+2.25Si

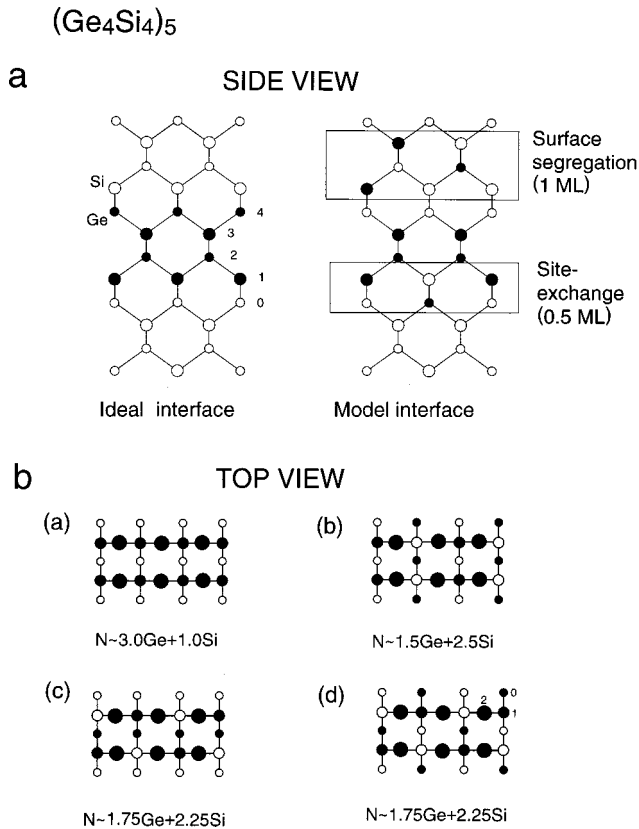FIG. 5. (a) Schematic side views of $(Ge_4Si_4)_5$ MSLS with an ideally sharp Ge/Si interface (left) and model structure (right). Shaded circles indicate Ge atoms and open circles indicate Si atoms. 1–4 layers denote the original Ge overlayers and 0 indicates the top layer of Si substrate (b) schematic plan view of Ge/Si interface of Ge overlayers on Si(001) with no site exchange (a) and with $\frac{1}{2}$ ML Ge-Si site exchange (b)–(d).

As can be seen, the best agreement is achieved for N_{Ge} = 1.8 and N_{Si} = 2.2. These values are close to those determined by the least-squares fit for all parameters, i.e., N, R and mean-square relative displacement (MSRD).

Figure 5(a) illustrates the schematic structures for $(Ge_4Si_4)_5$ MSLS with an ideal Ge/Si interface (left) and with an interface mixing (right). In the latter model, the Ge overlayer is assumed to have 0.5 ML site exchange upon deposition and 1 ML segregation upon Si overlayer growth. Figure 5(b) illustrates the schematic presentations of the interface local structure for the first Ge layer deposited on Si(001) with and without a site exchange effect. (a) shows the ideal interface while (b)–(d) are model interface structures where $\frac{1}{2}$ ML Ge sites exchange with Si atoms. Note that the site exchange decreases the N_{Ge}/N_{Si} ratio depending on which sites are involved, although (c) and (d) give the same value. In Fig. 6, we plot the RDF curves for the Ge-Ge and Ge-Si pairs for those model structures where 1 ML Ge is assumed to be segregated. The experimentally determined R_{Ge} and R_{Si} values are used in the simulation of RDF.

IV. DISCUSSION

For Ge overlayers grown on Si(001), a biaxial compression due to a lattice mismatch (4%) between Ge and Si causes a tetragonal deformation (elongation) of unit cell. Lat-
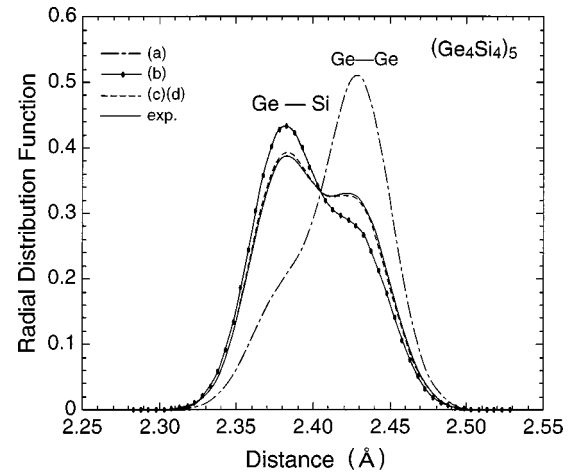

FIG. 6. Radial distribution functions for model interface structures. A solid line indicates that of experimental model independent results, while (a)–(d) correspond to the model structures in Fig. 5(b).

tice distortion is achieved by both bond bending and bond shortening for the Ge-Ge and Ge-Si pairs. Previous model structures of $(Ge_4Si_4)_5$ MSLS, however, assumed that the Ge-Si interface is atomically sharp, and described the tetragonal deformation with a macroscopic elastic theory. This is based on the assumption that only the Ge layers are deformed along the c axis, and ab plane lattice spacings (a = 5.43 Å, b = 5.43 Å) is kept constant. On the other hand, the c-axis lattice spacing $2c = 11.24$ Å expands by 0.38 Å compared with the $2c = 10.86$ Å of c-Si.[3]

The fact that band calculations based on this model structure could not explain a large oscillator strength observed for MSLS has been a puzzling question for a long time. Hybertsen and Schluter[19] have interpreted the strong optical transition (0.75 eV) observed in $(Ge_4Si_4)_5$ MSLS as an indirect transition based on the local-density-functional and quasiparticle self-energy approach using an ideal strained-layer superlattice structure with a sharp interface and strain confinement in the Ge layer. Ciraci and Batra,[6] have studied the stability and electronic properties of the strained Ge_nSi_n MSLS and Ge_xSi_{1-x} alloys using a self-consistent-field pseudopotential approach. Their results showed that Ge_nSi_n MSLS ($n=1,6$) are essentially unstable and the energy gap is indirect, although the separation between the direct and indirect gap is only 0.07 eV for $n=6$. People and Jackson have pointed out that the lowest-lying states (0.75, 1.25, and 2.31 eV) in the conduction band are derived from the (100) valleys of Si, but the magnitude of the matrix elements are several orders lower than what is observed in experiment.

On the contrary, Wong et al.[9] have predicted that optical transitions (0.9, 1.4, 2.3 eV) become direct if a fully relaxed Ge-Ge distance (2.45 Å) is assumed in their pseudopotential calculations of the electronic structure of $(Ge_4Si_4)_5$ MSLS. However, since these calculations are based on the model structures that are not established, and also the nature of transition would be sensitive to symmetry breaking by both local distortion and chemcal disorder, it is essential to investigate the local structure of Ge layers to evaluate these effects.

We have carried out the least-squares curve fit analysis

with structural parameters (N, R, and σ) for the two shells (Ge-Ge and Ge-Si), with a constraint on N, i.e., a tetrahedral coordination ($N_{Ge}+N_{Si}=4$). Here, N, R, and σ are coordination number, bond length, and square root of MSRD, respectively. In total, five parameters were varied until the best fit is obtained. The best-fit combination of coordination numbers ($N_{Ge}=1.8$, $N_{Si}=2.2$) is more Si-rich than that of an ideal interface model, i.e., $N_{Ge}=3$, $N_{Si}=1$. The uniqueness of structural parameters is guaranteed by the fact that the backscattering amplitude functions for Ge and Si scatterers are quite different, i.e., the low-k region is quite sensitive to the choice of N_{Ge}/N_{Si} ratio. In Fig. 4, simulated EXAFS curves for deliberately fixed values of N_{Ge}/N_{Si} ratio are compared with the results for all parameters least-square-fit. Therefore, we concluded that the average coordination numbers for Ge atoms in MSLS, which are model independent, are 1.8 ± 0.2 Ge and 2.2 ± 0.2 Si.

As can be seen in Table I, we find that the bond lengths R_{Ge-Ge} (2.42 Å) and R_{Ge-Si} (2.38 Å) in $(Ge_4Si_4)_5$ MSLS are slightly shorter than those of c-Ge ($R_{Ge-Ge}=2.45$ Å) and the sum of covalent radii ($R_{Ge-Si}=2.40$ Å). Hitchcock et al. and Aebi et al.[37,38] studied the local structures of the strained-layer $[(Si)_8(Ge)_2]_{100}$ and $[(Si)_9(Ge)_4]_{24}$ superlattices grown at 385 °C. They reported $R_{Ge-Ge}=2.413$ Å and $R_{Ge-Si}=2.388$ Å for $[(Si)_8(Ge)_2]_{100}$ superlattice, $R_{Ge-Ge}=2.403$ Å and $R_{Ge-Si}=2.394$ Å for $[(Si)_9(Ge)_4]_{24}$ superlattice. The bond lengths in $[(Si)_8(Ge)_2]_{100}$ superlattice are in good agreement with that of $(Ge_4Si_4)_5$ MSLS in Table I. More recently, we found that the bond length R_{Ge-Si} is 2.38 Å for the dilute Ge atoms doped into Si crystal.[39] This shows that the bond length $R_{Ge-Si}=2.38$ Å in $(Ge_4Si_4)_5$ MSLS takes the dilute limit value, suggesting that the contribution of bond-length compression is apparently $\frac{1}{4}$ but takes the upper limit of isotropic deformation. This is reasonable since above a certain bond-length compression limit, the strong repulsion is expected, and the deformation becomes unstable. Mousseau and Thorpe have calculated the Ge-Ge and Ge-Si bond lengths in crystalline and amorphous Ge_xSi_{1-x} alloys using Kirkwood potential.[29] The Ge-Ge and Ge-Si bond-length values $R_{Ge-Ge}=2.423$ Å and $R_{Ge-Si}=2.392$ Å calculated for $Ge_{0.55}Si_{0.45}$ are in agreement with the EXAFS results for $Ge_{0.5}Si_{0.5}$ alloy within an experimental error. Finally, we compare the present results with the experimental bond-length values for Ge_xSi_{1-x} alloys.[12–15,25–30] In spite of scatters in the reported bond-length values, the overall behaviors indicate a linear dependence on composition with a slope in agreement with elastic theory simulations. The observed R_{Ge-Ge} and R_{Ge-Si} values deviate from the experimental[12–15,25–30] or calculated[29,30] values for Ge_xSi_{1-x} alloys with the corresponding average composition ($x=0.45$). This suggests that the Ge layers and Ge-Si interface are both compressed, in agreement with the view that the strain is localized within the Ge layers.[3,4] On the other hand, they take slightly larger values than the calculated values for model Ge_4Si_4 MSLS.[6,10,16,18,19] The overestimation of bond-length compression may occur since most of model structures do not take interface mixing and nonuniform longitudinal displacement into account. Based on these, we may conclude that the lattice matching is achieved by tetragonal deformation by bond bending but the Ge layer is highly compressed. In an interface region, the magnitude of local lattice distor-

tion indeed amounts to the same with that of a dilute limit (under isotropic compression).[39]

In summary, $\frac{1}{4}$ of the mismatch strain in $(Ge_4Si_4)_5$ MSLS is accommodated by the Ge-Ge bond-length variation while $\frac{3}{4}$ is compensated by bond bending, in agreement with the bond-length values of GeSi alloys[12–15,25–30] that are linearly dependent on composition. Second, the observed R_{Ge-Ge} and R_{Ge-Si} values of MSLS rule out a possible model structure in which R_{Ge-Ge} is fully relaxed. Thus, the energy level lowering due to the relaxed Ge-Ge bond length is not likely the case. Third, the observed ratio of Ge and Si coordination number in $(Ge_4Si_4)_5$ MSLS reveals that the Ge-Si mixing occurs at the interface as reported earlier for Ge overlayers on Si(001) (Ref. 23) although the cross-section transmission microscopy shows that the (Ge_4) layers are clearly separated from (Si_4) layers.[3] There are two factors to be considered that contribute to the interface mixing: the site exchange during the Ge layer deposition on Si surface and the surface segregation during the Si overlayer growth on Ge layers. Our XAFS studies of Ge epitaxial overlayers on well-oriented Si(001) [Ge_n/Si(001), $n<7$] have shown that $\sim\frac{1}{2}$ ML of Ge atoms in the first deposited layer are replaced by the substrate Si atoms relieving elastic strain in the second layer caused by a large atomic size mismatch between the adatom (Ge) and substrate atoms (Si) and bond bending due to dimers.[23] In the present study, we assume that the Ge-Si interface mixing during the Ge growth on Si(001) is also about $\frac{1}{2}$ Ge ML. Two models of Ge/Si site-exchange during the Ge overlayer growth, (b) and (c) or (d) are shown in Fig. 5(b). In this figure, we consider four layers, i.e., the larger circles (3, 2) indicate the top- and second-layer atoms while the small open circles (1, 0) indicate the third- and fourth-layer atoms. As illustrated in the figure, the average Ge coordination number N_{Ge} decreases from 3.0 in (a) to 1.5–1.75 in (b)–(d) as the site exchange occurs.

For the Si growth on the Ge layer, the Ge atoms are pumped up to the top layer (surface segregation) that eventually introduces the Ge/Si mixing. Based on the separate XAFS experiments on the effect of of Si growth on the Ge layer,[40] we estimate that about 1 ML of Ge atoms migrate to the top layer. Assuming that the segregated atoms are surrounded by Si atoms, we calculated the average RDF curves for the Ge-Ge and Ge-Si pairs for $(Ge_4Si_4)_5$ MSLS and compared them with the experimental RDF in Fig. 6. The RDF was generated by Gaussian distribution function using the model-independent bond lengths determined by a curve-fit analysis of EXAFS data.

As illustrated in Fig. 6, the experimental RDF fits well to model (c) or (d). The detail of the in situ XAFS study on Ge overlayers on Si(001) is reported elsewhere.[41] The nominal composition $Ge_{0.44}Si_{0.56}$ for model (c) or (d) is close to that of $(Ge_4Si_4)_5$ MSLS, i.e., $Ge_{0.45}Si_{0.55}$. Although whether the interface has an ordered structure or not is not experimentally established yet, we believe that the interface mixing is roughly explained by the two contributions, i.e., Ge-Si site-exchange and Ge surface segregation. We note that the site exchange is hardly explained in terms of thermally activated diffusion.

Two factors influencing the optical transition are considered. First, the interface-mixing (chemical and structural disorder) would relax the k-conservation rule that may increase

the transition matrix element. Second, the GeSi alloy interface can be an intermediate ''buffer'' between Ge and Si layers helping the flat layer-by-layer growth. This would decrease the localized strain contributing to stabilize the MSLS, which may increase the gap energy. As a result normally inhibited direct transition might be allowed or the weak indirect transition might be enhanced on the contrary.

V. CONCLUSION

Grazing-incidence fluorescence XAFS has been used to study the local structures of $(Ge_4Si_4)_5$ MSLS. The bond length values for the Ge-Ge and Ge-Si pairs ($R_{Ge-Ge} = 2.42$ Å, $R_{Ge-Si} = 2.38$ Å) indicate that the proposed model[9] with fully relaxed Ge-Ge bond length is not appropriate. The determined Ge/Si coordination number ratio N_{Si}/N_{Ge} (1.22)

is smaller than the ideal value (3), indicating a significant degree of interface mixing. A model structure based on a site-selective Ge-Si exchange at the interface and surface segregation is proposed to explain the EXAFS results. The realistic band calculation to investigate the origin of an optical transition (0.75 eV) should take into account the local structure of Ge layers that are not relaxed but strained and disorder effects due to the interface mixing.

*FAX: (81) 298-61-5085. Electronic address: sqwei@etl.go.jp

[1] J. C. Bean, L. C. Feldman, A. T. Fiory, S. Nakahara, and I. K. Robinson, J. Vac. Sci. Technol. A **2**, 436 (1984).

[2] H. Temkin, T. P. Pearsall, J. C. Bean, R. A. Logan, and S. Luryi, Appl. Phys. Lett. **48**, 963 (1986).

[3] T. P. Pearsall, J. Bevk, L. C. Feldman, J. M. Bonar, J. P. Mannaerts, and A. Ourmazd, Phys. Rev. Lett. **58**, 729 (1987).

[4] T. P. Pearsall, F. H. Pollak, J. C. Bean, and R. Hull, Phys. Rev. B **33**, 6821 (1986).

[5] J. Bevk, J. P. Mannaerts, L. C. Feldman, B. A. Davidson, and A. Ourmazd, Appl. Phys. Lett. **49**, 286 (1986).

[6] S. Ciraci and P. Batra, Phys. Rev. B **38**, 1835 (1988).

[7] T. P. Pearsall, J. Bevk, J. C. Bean, J. Bonar, J. P. Mannaerts, and A. Ourmazd, Phys. Rev. B **39**, 3741 (1989).

[8] T. P. Pearsall, Appl. Phys. Lett. **60**, 1712 (1992).

[9] K. B. Wong, M. Jaros, I. Morrison, and J. P. Hagon, Phys. Rev. Lett. **60**, 2221 (1988).

[10] S. Satpathy, R. M. Martin, and Van de Walle, Phys. Rev. B **38**, 13 237 (1988).

[11] H. Oyanagi, K. Sakamoto, R. Shioda, Y. Kuwahara, and K. Haga, Phys. Rev. B **52**, 5824 (1995).

[12] D. B. Aldrich, R. J. Nemanich, and D. E. Sayers, Phys. Rev. B **50**, 15 026 (1994).

[13] C. Woicik, K. E. Miyano, C. A. King, R. W. Johnson, J. G. Pellegrino, T.-L. Lee, and Z. H. Lu, Phys. Rev. B **57**, 14 592 (1998).

[14] J. C. Aubry, T. Tyliszczak, and A. P. Hitchcock, Phys. Rev. B **59**, 12 872 (1999).

[15] M. C. Ridgway, K. M. Yu, C. J. Glover, G. J. Foran, C. Clerc, J. L. Hansen, and A. Nylandsted Larsen, Phys. Rev. B **60**, 10 831 (1999).

[16] M. Ikeda, K. Terakura, and T. Oguchi, Phys. Rev. B **48**, 1571 (1993).

[17] R. People and S. Jackson, Phys. Rev. B **36**, 1310 (1987).

[18] C. Ciraci and I. P. Batra, Phys. Rev. Lett. **58**, 2114 (1987).

[19] M. S. Hybertsen and M. Schluter, Phys. Rev. B **36**, 9683 (1987).

[20] I. Morrison, M. Jaros, and K. B. Wong, Phys. Rev. B **37**, 9693 (1987).

[21] H. Oyanagi, R. Shioda, Y. Kuwahara, and K. Haga, J. Synchrotron Radiat. **2**, 99 (1995).

[22] L. M. Murphy, B. R. Dobson, M. Neu, C. A. Ramsdale, R. W. Strange, and S. S. Hasnain, J. Synchrotron Radiat. **2**, 64 (1995).

[23] H. Oyanagi, K. Sakamoto, R. Shioda, and T. Sakamoto, Jpn. J. Appl. Phys. **33**, 3515 (1994).

[24] H. Oyanagi, K. Sakamoto, and T. Sakamoto, Jpn. J. Appl. Phys., Suppl. **32**, 119 (1993).

[25] J. C. Woicik, C. E. Bouldin, M. I. Bell, J. O. Cross, D. J. Tweet, B. D. Swanson, T. M. Zhang, L. B. Sorensen, C. A. King, J. L. Hoyt, P. Pianetta, and J. F. Gibbons, Phys. Rev. B **43**, 2419 (1991).

[26] J. C. Woicik, C. E. Bouldin, K. E. Miyano, and C. A. King, Phys. Rev. B **55**, 15 386 (1997).

[27] M. Matsuura, J. M. Tonnerre, and G. S. Cargill III, Phys. Rev. B **44**, 3842 (1991).

[28] H. Kajiyama, S. Muramatsu, T. Shimada, and Y. Nishino, Phys. Rev. B **45**, 14 005 (1992).

[29] N. Mousseau and M. F. Thorpe, Phys. Rev. B **46**, 15 887 (1992).

[30] M. Laradji and D. P. Landau, Phys. Rev. B **51**, 4894 (1995).

[31] T. P. Pearsall, J. Bevk, J. C. Bean, J. Bonar, and J. P. Mannaerts, Phys. Rev. B **39**, 3741 (1989).

[32] K. Sakamoto, T. Sakamoto, S. Nagao, G. Hashiguchi, K. Kuniyoshi, and Y. Bando, Jpn. J. Appl. Phys. **26**, 666 (1987).

[33] H. Oyanagi, Y. Kuwahara, and H. Yamagushi, Rev. Sci. Instrum. **66**, 4482 (1995).

[34] D. W. Marquardt, J. Soc. Ind. Appl. Math. **11**, 431 (1963).

[35] J. J. Rehr, S. I. Zabinsky, and R. C. Albers, Phys. Rev. Lett. **69**, 3397 (1992).

[36] D. E. Sayers and B. A. Bunker, in *X-ray Absorption, Principles, Applications, Techniques of EXAFS, SEXAFS and XANES*, edited by D. C. Koningsberger and R. Prins (Wiley, New York, 1988), p. 211.

[37] A. P. Hitchcock, T. Tyliszczak, P. Aebi, J. Z. Xiong, T. K. Sham, K. M. Baines, K. A. Mueller, X. H. Feng, J. M. Chen, B. X. Yang, Z. H. Lu, J.-M. Baribeau, and T. E. Jackman, Surf. Sci. **291**, 349 (1993).

[38] P. Aebi, T. Tyliszczak, A. P. Hitchcock, K. M. Baines, T. K. Sham, T. E. Jackman, J. M. Baribeau, and D. J. Lockwood, Phys. Rev. B **45**, 13 579 (1992).

[39] S. Q. Wei, H. Oyanagi, H. Kawanami, K. Sakamoto, T. Sakamto, K. Tamura, N. L. Saini, and K. Uosaki, J. Appl. Phys. **82**, 4810 (1997).

[40] H. Oyanagi (unpublished).

[41] H. Oyanagi and K. Sakamoto (unpublished).